Impact of Cu,Zn-Superoxide Dismutase and Se-Dependent Glutathione Peroxidase-1 Knockouts on Acetaminophen-Induced Cell Death and Related Signaling in Murine Liver

JIAN-HONG ZHU, XIAOMEI ZHANG, JAMES P. MCCLUNG, AND XIN GEN LEI[1]
Department of Animal Science, Cornell University, Ithaca, New York 14853

There is increasing evidence showing dual functions of antioxidant enzymes in coping with reactive oxygen species (ROS) versus reactive nitrogen species (RNS). The objective of this study was to compare the impacts of knockout of Cu,Zn-superoxide dismutase (SOD1) and Se-dependent glutathione peroxidase-1 (GPX1) on cell death and related signaling mediated by acetaminophen (APAP), a RNS inducer in liver. Two groups of young adult knockout mice ($SOD1^{-/-}$ and $GPX1^{-/-}$), along with their wild types (WT), were killed 5 hrs after an ip injection of saline or APAP (300 mg/kg body wt). While the WT mice showed more hepatic necrosis and DNA breakage than the $GPX1^{-/-}$ mice, the $SOD1^{-/-}$ mice had essentially no positive response compared with their saline-injected controls. The APAP treatment activated liver c-jun N-terminal kinase (JNK) in the WT and $GPX1^{-/-}$ mice, but not in the $SOD1^{-/-}$ mice. The APAP-induced changes in other cell death–related signal proteins such as p21, caspase-3, and poly(ADP-ribose) polymerase (PARP) also were obviated in the $SOD1^{-/-}$ mice. In conclusion, knockout of GPX1 did not potentiate APAP-induced cell death and related signaling, whereas the SOD1 null blocked APAP-induced hepatic JNK phosphorylation and cell death. Exp Biol Med 231:1726–1732, 2006

Key words: acetaminophen; cell death; glutathione peroxidase; oxidative stress; signaling; superoxide dismutase

Introduction

Aerobic metabolism constantly produces reactive oxygen species (ROS) and reactive nitrogen species (RNS; Ref. 1). Excessive production of ROS and RNS causes oxidative stress, leading to destruction of macromolecules and cell death (1). Cu,Zn-superoxide dismutase (SOD1) and Se-dependent cellular glutathione peroxidase-1 (GPX1) are considered two primary intracellular antioxidant enzymes in mammals. By converting superoxide anions into the substrate of GPX1, hydrogen peroxide, SOD1 actually functions upstream of GPX1. Because of this coupled action, SOD1 and GPX1 have been perceived as performing similar functions in coping with oxidative stress. Indeed, both enzymes protect against ROS-related oxidative stress (2, 3). Knockout of either enzyme renders animals susceptible to oxidative injuries or cell death mediated by ROS generators, such as diquat (4–7).

As a widely used analgesic and antipyretic drug, acetaminophen (APAP) overdose represents the leading drug poison in the United States today (8). The median dose of unintentional overdoses is approximately 11.5 g, compared with 20 g for suicidal patients (8). It has been shown that high levels of APAP induce RNS (peroxynitrite) formation and hepatic protein nitration (9–11). However, the impacts of GPX1 and SOD1 on APAP toxicity have been intriguing. Following a lethal dose of APAP (425 mg/kg), mice overexpressing SOD1 had extended survival times, whereas mice overexpressing human GPX1 had accelerated death and aggravated hepatotoxicity, compared with wild-type (WT) mice (12). While administration of SOD1 enzyme or mimic also offered protection against APAP overdose (13, 14), the GPX1 null mice were partially protected from APAP-induced plasma alanine aminotransferase (ALT) activity increases, a hallmark of APAP-induced liver injury (11). GPX1 and SOD1 seemingly exerted opposite effects on APAP-mediated toxicity. Apparently, GPX1 and SOD1 null mice are better models than the GPX1 and SOD1 overexpressed mice to study the physiologic roles of these two enzymes in APAP overdose. However, such impacts of SOD1 and GPX1 null have not been compared at the exact same experimental conditions.

Oxidative stress–mediated cell death often involves c-jun N-terminal kinase (JNK) and p38 mitogen-activated protein kinase (p38) phosphorylation, mitochodrial dys-

This study was supported by National Institutes of Health grant DK53108 to X.G.L.

[1] To whom correspondence should be addressed at Cornell University, 252 Morrison Hall, Ithaca, NY 14853. E-mail: XL20@cornell.edu

Received March 7, 2006.
Accepted May 8, 2006.

1535-3702/06/23111-1726$15.00

function and release of cytochrome *c*, and proteolytic cleavage of caspases (15–19). A number of signaling pathways, including mitochondria-mediated pathways and mitogen-activated protein kinases, have been shown to be involved in APAP-induced mitochondrial dysfunction and cell death (20–25). In C6 glioma cells, JNK-related cell death pathway was activated by APAP (20). It also has been shown that APAP induces the expression of p21 (23), modification of Bcl-X_L (26), and the activation of caspase-3 that results in cleavage of poly(ADP-ribose) polymerase (PARP; Refs. 21, 24, 27). To the best of our knowledge, no study has been reported to compare the effects of GPX1 and SOD1 knockout on hepatic cell death signaling caused by oxidative stress in general or APAP toxicity in particular. Therefore, we challenged the GPX1 knockout mice ($GPX1^{-/-}$), SOD1 knockout mice ($SOD1^{-/-}$), and their WT mice with an ip injection of APAP (300 mg/kg body wt). Our objective was to compare the impacts of these two major antioxidant enzymes on APAP-induced hepatic cell death, DNA breakage, and the related signaling.

Materials and Methods

Chemicals and Antibodies. All chemicals were purchased from Sigma Chemical Co. (St. Louis, MO) unless otherwise indicated. JNK2 and p21 were from Santa Cruz Biotechnology (Santa Cruz, CA); caspase-3 and IκBε were from Transduction Laboratories (Lexington, KY); phospho-JNK (Thr183/Tyr185), phospho-p38, and p38 were from Cell Signaling (Beverly, MA); Bcl-X was from Pharmingen (San Diego, CA); PARP was from Chemicon (Temecula, CA); anti-rabbit IgG was from Bio-Rad Laboratories (Hercules, CA); and anti-mouse IgG was from Pierce (Rockford, IL). Notably, the JNK2 antibody recognizes both JNK1 and JNK2. The phospho-JNK antibody recognizes both phosphorylated JNK1 and JNK2.

Animals and Treatments. Our experiments were approved by the Institutional Animal Care and Use Committee at Cornell University and were conducted in accordance with the National Institutes of Health guidelines for animal care. The $GPX1^{-/-}$, $SOD1^{-/-}$, and WT mice were generated from 129SVJ × C57BL/6 mice (5, 6). All mice were 8–10 weeks old and were fed an Se-adequate (0.4 mg/kg) diet. All of the genotype mice were injected ip with phosphate-buffered saline (PBS) or APAP (300 mg/kg body wt) ($n = 6$ per genotype by treatment) and were euthanized at 5 hrs after injection. The APAP dose was close to the suicidal dose in humans (20 g per 65 kg body wt; Ref. 8).

Liver Injury Assay and Immunohistochemistry. Blood and tissue samples were collected immediately after mice were anesthetized with carbon dioxide and killed by heart puncture. The plasma was used for determination of ALT activity using the Sigma ALT 10 kit. For histologic analysis, liver samples were formalin fixed, paraffin embedded, and sectioned as described previously (15). Replicate sections were stained with hematoxylin and eosin. Hepatic DNA strand breaks were detected using an ApopTag plus kit (Intergen, Norcross, GA). Briefly, residues of digoxigenin nucleotides were added to DNA ends by terminal deoxynucleotidyl transferase (TUNEL) assay, and then marked nucleotides were visualized using a peroxidase-labeled antidigoxigenin antibody.

Biochemical Analyses. Total GPX activity was measured by the coupled assay of NADPH oxidation using hydrogen peroxide as substrate (28). The enzyme activity is expressed as nanomoles of glutathione oxidized per minute per milligram of protein. Total SOD activity was measured using a water-soluble formazan dye kit (Dojindo Molecular Technologies, Gaithersburg, MD).

Western Blot Analyses. Liver samples were homogenized (Polytron PT3100; Brinkmann Instruments, Littau, Switzerland) in either buffer I (50 m*M* Hepes, pH 7.4; 100 m*M* NaCl; 1% Triton X-100; 5 m*M* EDTA; 1 m*M* sodium pyrophosphate; 1 m*M* sodium orthovanadate; 1 m*M* NaF; 1 m*M* phenylmethylsulfonyl fluoride; 10 μg/ml leupeptin; 10 μg/ml aprotinin; 1 μ*M* microcystin) for Western blot analyses of phospho-p38 and phospho-JNK, or in buffer II (50 m*M* potassium phosphate buffer, pH 7.8; 0.1% Triton X-100; 1.34 m*M* diethylenetriaminepentaacetic acid; 1 m*M* phenylmethylsulfonyl fluoride; 10 μg/ml peptstain A; 10 μg/ml leupeptin; 10 μg/ml aprotinin) for Western blot analyses of other proteins. The homogenates were centrifuged at 14,000 *g* for 20 mins at 4°C. Protein concentration in buffer I was measured with a BCA protein assay kit (Pierce Chemical Co., Rockford, IL). Protein concentration in buffer II was measured by Lowry method (29). The supernatant (20 or 50 μg protein per lane) was loaded for Western blot analyses, and the bands were detected with SuperSignal West Pico Kit (Pierce Chemical Co.) according to the manufacturer's instructions. After detection of a specific protein, the same blot was stripped and reprobed against vinculin antibody (Sigma) to normalize loading.

Statistical Analysis. Data were analyzed using the general linear model procedure in SAS (release 6.11; SAS Institute, Cary, NC) as a one-way analysis of variance. Significance was defined as $P < 0.05$.

Results

Liver GPX1 and Total SOD Activity. Compared with WT, $GPX1^{-/-}$ mice had only 0.34% of GPX1 activity in liver, and $SOD1^{-/-}$ mice had only 0.9% of total SOD activity (Table 1). Hepatic GPX1 activity was reduced by 46% ($P < 0.05$) in the $SOD1^{-/-}$ mice compared with WT mice. The APAP treatment led to a 62% ($P < 0.05$) loss of GPX1 activity in WT mice but no significant decrease in $SOD1^{-/-}$ mice. The APAP treatment also caused a 44% ($P < 0.05$) reduction in total SOD activity in $GPX1^{-/-}$ mice but not in WT mice.

Knockout of SOD1 or GPX1 on APAP-Induced Liver Injury. The APAP treatment caused plasma ALT

Table 1. Effect of Genotypes and Acetaminophen (APAP) Treatment on Activities of Plasma Alanine Aminotransferase (ALT) and Hepatic Glutathione Peroxidase-1 (GPX1) and Total Superoxide Dismutase (SOD)[a]

	Wild type		$GPX1^{-/-}$		$SOD1^{-/-}$	
	PBS	APAP	PBS	APAP	PBS	APAP
Plasma ALT activity (U/l)	14 ± 3	1964 ± 775[b]	16 ± 4	1045 ± 383[b]	16 ± 7	63 ± 13[b,c]
Liver GPX1 activity (U/mg protein)	1057 ± 22	400 ± 51[b]	4 ± 1[c]	2 ± 1[c]	572 ± 170[c]	453 ± 34
Liver SOD activity (U/mg protein)	1427 ± 58	1346 ± 108	1314 ± 125	741 ± 63[b,c]	13 ± 3[c]	13 ± 2[c]

[a] Mice were treated with phosphate-buffered saline (PBS) or APAP (300 mg/kg) for 5 hrs. Values are mean ± SE ($n = 6$).
[b] APAP treatment effect ($P < 0.05$) compared with PBS treatment within genotypes.
[c] Genotype effect ($P < 0.05$) compared with wild type within the same treatment.

activity increases ($P < 0.05$) in all genotypes. However, the increase was highest in WT mice and lowest in $SOD1^{-/-}$ mice ($P < 0.05$; Table 1). Both WT and $GPX1^{-/-}$ mice showed more severe hepatocyte necrosis than $SOD1^{-/-}$ mice (Fig. 1). The livers of PBS-treated controls of all three genotypes were histologically normal (Fig. 1A, C, and E). Typical signs of necrosis and hemorrhages were shown in central lobular areas of the APAP-treated WT and $GPX1^{-/-}$ mice, including cloudy swelling and fatty/vacuolar degeneration of the surviving cells on the border and/or within the lesion (Fig. 1B and D). Hepatocytes in the APAP-treated $SOD1^{-/-}$ mice were largely unaffected (Fig. 1F). DNA strand breaks were readily seen in TUNEL-stained hepatocytes (brown color) in WT and $GPX1^{-/-}$ mice (Fig. 2B and D), but hardly in the $SOD1^{-/-}$ mice (Fig. 2F). The livers of PBS-treated controls of all three genotypes were virtually no staining (Fig. 2A, C, and E). APAP treatment produced strong staining in both the cytoplasm and nucleus of hepatocytes of WT mice, and staining was particularly intense around the central veins (Fig. 2B). In contrast, there was less intense staining in $GPX1^{-/-}$ mice (Fig. 2D).

Knockout of GPX1 or SOD1 on APAP-Mediated Signaling. There were no significant baseline differences

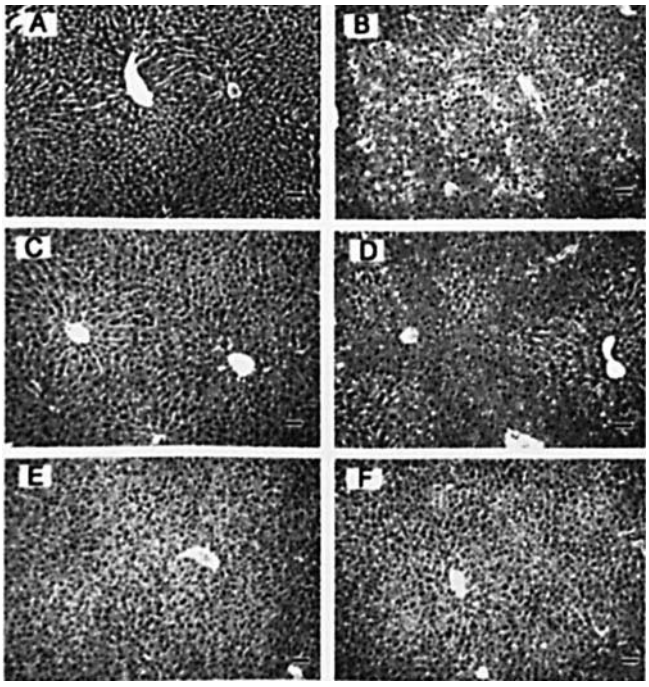

Figure 1. Effect of knockout of glutathione peroxidase-1 (GPX1) and Cu,Zn-superoxide dismutase (SOD1) on acetaminophen (APAP)–induced hepatic lesions. Liver samples were collected from wild-type (A and B), $GPX1^{-/-}$ (C and D), or $SOD1^{-/-}$ (E and F) mice 5 hrs after the mice were treated with phosphate-buffered saline (A, C, and E) or APAP (300 mg/kg; B, D, and F). The samples were formalin fixed, paraffin embedded, sectioned, and stained with hematoxylin and eosin. The morphologic characteristic was visualized under light microscopy (original magnification: ×100). The image is representative of five sets of data.

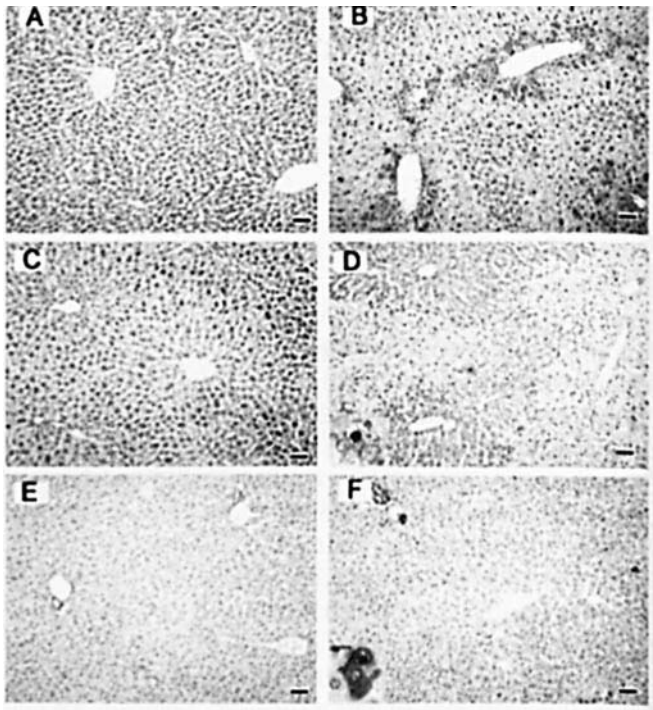

Figure 2. Effect of knockout of glutathione peroxidase-1 (GPX1) and Cu,Zn-superoxide dismutase (SOD1) on acetaminophen (APAP)–induced hepatic DNA strand breaks. Liver samples were collected from wild-type (A and B), $GPX1^{-/-}$ (C and D), or $SOD1^{-/-}$ (E and F) mice 5 hrs after the mice were treated with phosphate-buffered saline (A, C, and E) or APAP (300 mg/kg; B, D, and F), and they were formalin fixed, paraffin embedded, and sectioned. Hepatic DNA strand breaks were assessed using an ApopTag plus kit. The brown color shows a positive response (original magnification: ×100). The image is representative of five sets of data. Arrow points to cells with brown staining (original magnification: ×400).

in nine signal proteins among the WT, GPX1$^{-/-}$, and SOD1$^{-/-}$ mice treated with PBS (Figs. 3 and 4). APAP treatment did not activate liver p38 MAPK, but it activated liver JNK (p46-JNK1 and p54-JNK2) at Thr183 and Tyr185 in WT and GPX1$^{-/-}$ mice ($P < 0.05$; Fig. 3). However, the APAP-induced phosphorylation of hepatic JNK was not seen in SOD1$^{-/-}$ mice (Fig. 3). APAP treatment caused the cleavage of caspase-3 from a 32-kDa proform to a 24-kDa active form in WT and GPX1$^{-/-}$ mice ($P < 0.05$), but not in the SOD1$^{-/-}$ mice (Fig. 4). Intact PARP, a nuclear enzyme involved in DNA repair and stability, was seen in PBS-treated mice. The APAP treatment resulted in a greater upregulated expression of PARP and a stronger cleavage of the 85-kDa band in WT and GPX1$^{-/-}$ mice than in SOD1$^{-/-}$ mice ($P < 0.05$). Compared with their respective PBS-treated controls, hepatic IκBε, Bcl-X_L, and p21 proteins were reduced ($P < 0.05$) in APAP-treated WT and/or GPX1$^{-/-}$ mice ($P < 0.05$). In contrast, there was no such change of these proteins in APAP-treated SOD1$^{-/-}$ mice (Fig. 4).

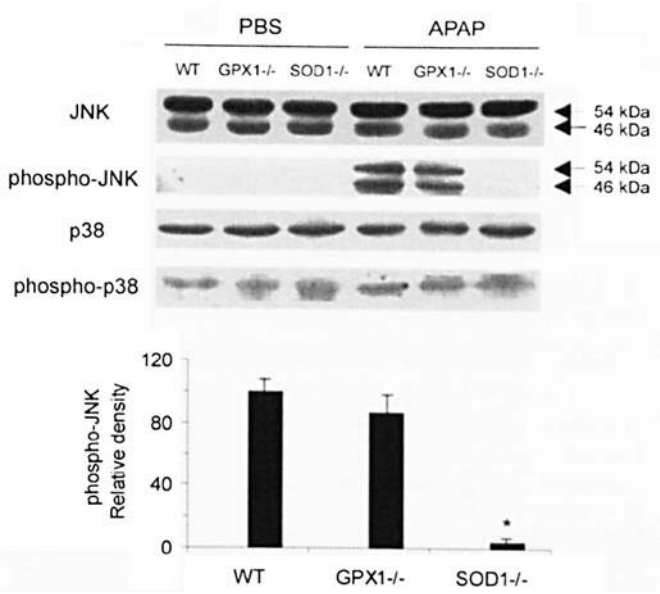

Figure 3. Western blot analysis of knockout of glutathione peroxidase-1 (GPX1) and Cu,Zn-superoxide dismutase (SOD1) on acetaminophen (APAP)–induced responses of liver c-jun N-terminal kinase (JNK), phospho-JNK, mitogen-activated protein kinase p38 (p38), and phospho-p38. Liver samples were collected from wild-type, GPX1$^{-/-}$, or SOD1$^{-/-}$ mice 5 hrs after the mice were treated with phosphate-buffered saline or APAP (300 mg/kg), homogenized, and separated as described in the text. The upper panel shows representative blots of three independent analyses, and the lower panel shows bar graphs of the relative density of the phosphorylated JNK protein ($n = 3$) in the APAP-treated mice. *$P < 0.05$ versus WT.

Discussion

One of the most important findings from this study is that APAP-induced hepatic cell death was not potentiated by GPX1 null but was nearly completely blocked by SOD1 null. As in most studies (11, 30, 31), we have demonstrated liver necrosis and DNA strand breaks in APAP-treated WT mice. The lack of aggravated cell death and attenuated DNA damage after the APAP treatment in GPX1$^{-/-}$ mice compared with WT mice was consistent with plasma ALT activity changes observed by us and others (11). Previous studies have shown that overexpression of GPX1 sensitized mice to APAP-induced lethality (12), and knockout of GPX1 protected against peroxynitrite-induced apoptosis in primary hepatocytes (32) and kainic acid (RNS inducer)–induced seizers and lethality in mice (33). These results suggest a potential promoting role of GPX1 in RNS-related oxidative stress, and they do not support the previously proposed function of GPX1 as a peroxynitrite reductase (34).

The nearly completely blocked hepatic cell death and DNA breakage in APAP-treated SOD1$^{-/-}$ mice was in stark contrast to the observed protection conferred by SOD1 overexpression (12), enzyme (13), or mimic (14) against APAP overdose. Likewise, this suggests that the physiologic expression of SOD1 activity, unlike the pharmacologic levels of SOD1, does not protect against—if not promote—APAP-induced toxicity. It is interesting to note that SOD1 catalyzed peroxynitrite-mediated protein nitration *in vitro* (35), and overexpression of SOD1 promoted kainic acid–induced neuron apoptosis (36). Although the physiologic role of SOD1 in APAP-mediated protein nitration is still under active investigation in our laboratory, the present study clearly shows a stronger impact of SOD1 null than GPX1 null on drug-induced hepatic cell death and DNA strand breakage.

The impacts of SOD1 and GPX1 knockouts on cell survival and death-related signaling help explain the genotype differences in APAP-mediated cell death and DNA strand breakage. Similar to the results reported by Bae et al. (20), we have shown that hepatic JNK but not p38 MAPK was activated by APAP treatment at 5 hrs in WT mice. While GPX1$^{-/-}$ mice shared a similar extent of necrosis to that of WT after APAP injection, the two groups had similar levels of JNK phosphorylation. In contrast, SOD1$^{-/-}$ mice were largely protected from the APAP-induced cell death and DNA breakage, and they displayed no phosphorylation of JNK. Activated JNK inactivates Bcl-X_L, a member of bcl-2 family that blocks cell apoptosis (37). As p38 MAPK is not as efficient as JNK to phosphorylate bcl-2 (37), APAP-induced activation of JNK may be sufficient to initiate the cascade of hepatocyte apoptosis. Overexpression of Bcl-X_L has been shown to reduce APAP-induced apoptosis by blocking the release of cytochrome *c* from mitochondria, an event that induces the activation of caspase-3 (38). Besides the SOD1 null, the GPX1 null also seemed to prevent the downregulation or inactivation of Bcl-X_L induced by APAP. This effect might contribute to the partial protection against APAP-induced DNA breakage in GPX1$^{-/-}$ mice. However, it remains unclear to us how the GPX1 null exerted its impact on Bcl-

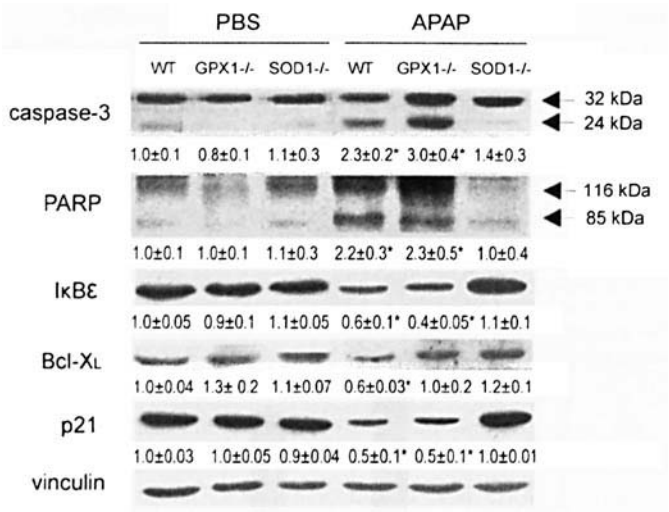

Figure 4. Western blot analysis of knockout of glutathione peroxidase-1 (GPX1) and Cu,Zn-superoxide dismutase (SOD1) on acetaminophen (APAP)–induced responses of liver caspase-3, poly(ADP-ribose) polymerase (PARP), IκBε, Bcl-X_L, and p21 protein levels. Liver samples were collected from wild-type, GPX1$^{-/-}$, or SOD1$^{-/-}$ mice 5 hrs after the mice were treated with phosphate-buffered saline (PBS) or APAP (300 mg/kg), homogenized, and separated as described in the text. Each panel shows representative blots of three independent analyses, and values underneath each band indicate the relative density ($n = 3$) compared with the PBS-treated WT. *$P < 0.05$ versus PBS-treated WT.

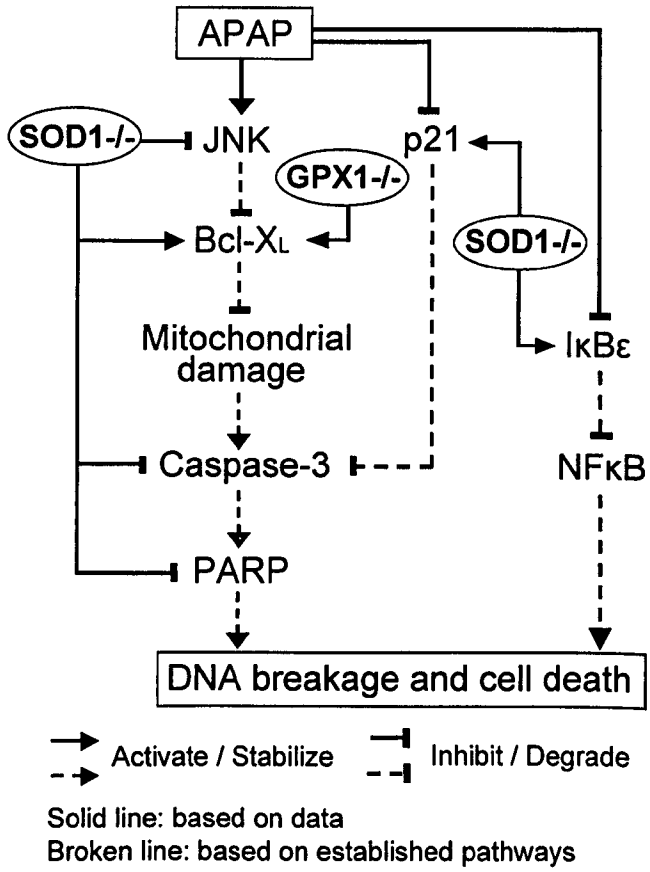

Figure 5. Schematic illustration of knockout of glutathione peroxidase-1 (GPX1) and Cu,Zn-superoxide dismutase (SOD1) on acetaminophen (APAP)–induced DNA breakage, cell death, and related signaling. JNK, c-jun N-terminal kinase; PARP, poly(ADP-ribose) polymerase.

X_L, whereas in SOD1$^{-/-}$ mice the action mode was likely via the block of JNK phosphorylation.

As previously reported (21), APAP induced activation of caspase-3 by proteolytic cleavage of pro-caspase-3 into p24-caspase-3, which initiated DNA fragmentation (15). Activated caspase-3 cleaved intact PARP to 85-kDa and 24-kDa fragments that no longer have normal enzymatic functions to repair damaged DNA or to maintain DNA stability (27). Consistently, the cleavage of PARP fragment was evident in WT and GPX1$^{-/-}$ mice in which caspase-3 was also activated. In contrast, there was little PARP cleave in the less caspase-3–activated SOD1$^{-/-}$ mice. Unlike the unanimous results on caspase-3 activation, the APAP-mediated responses of p21, a cyclin-dependent kinase inhibitor and an inhibitor of apoptosis, seem to be ambiguous. Chiu et al. (23) reported that APAP induced expression of p21, whereas others showed no alteration of p21 expression by APAP treatment (39). In the present study, we have found a repressed expression of p21 by APAP treatment in WT and GPX1$^{-/-}$ mice but not SOD1$^{-/-}$ mice. As p21 interacts with pro-caspase-3 and inhibits its conversion to the mature form (40), the repression of p21 in WT and GPX1$^{-/-}$ mice promoted the activation of caspase-3 in the two genotypes. We have shown that IκBε, one isoform of IκB, was degraded in WT and GPX1$^{-/-}$ mice, but not in the SOD1$^{-/-}$, by APAP treatment. The degradation of IκBε may contribute partially to the release of the inhibition on nuclear factor κB (NF-κB), which is deactivated by binding to IκB (41). NF-κB is known to be a major transcription factor regulating inducible nitric oxide synthase (iNOS) expression, leading to the production of nitric oxide. Indeed, APAP has been shown to induce the increased production of nitric oxide (9). Overall, the block of JNK phosphorylation and downregulation of p21 in APAP-treated SOD1$^{-/-}$ mice led to the inhibition of caspase-3 activation and PARP cleavage (Fig. 5). As these two events and DNA strand breaks are well-known characteristics of apoptotic cell death (27), and our histological data show typical signs of necrosis and hemorrhages in the central lobular of APAP-treated WT mice, it seems that the protection by SOD1 knockout against APAP-mediated hepatic cell death is involved in both apoptosis and necrosis. Again, the GPX1 null showed much less effect on these processes compared with the SOD1 null.

In summary, the present study indicates that knockout of SOD1 protected against APAP-induced hepatic cell death and related signaling, whereas knockout of GPX1 did not potentiate but offered partial protection against the insult. Apparently, physiologic expression of SOD1 or GPX1 was not critical or beneficial for the body to defend against this type of oxidative stress involved in RNS production. It is

also clear that the two major antioxidant enzymes did not exert the same impact on the drug-induced oxidative stress. Although SOD1 and GPX1 are considered major intracellular antioxidant enzymes, increasing evidence has suggested dual functions of these enzymes under different types of oxidative stress (11, 12, 32, 33, 36). Elucidating the mechanism for those potential pro-oxidant roles of GPX1 and SOD1 will enable us to understand the full array of functions of antioxidant enzymes in metabolism and help in developing new approaches for the therapy of diseases caused by drug toxicity or oxidative stress.

1. Inoue M, Sato EF, Nishikawa M, Park AM, Kira Y, Imada I, Utsumi K. Cross talk of nitric oxide, oxygen radicals, and superoxide dismutase regulates the energy metabolism and cell death and determines the fates of aerobic life. Antioxid Redox Signal 5:475–484, 2003.
2. Wang P, Chen H, Qin H, Sankarapandi S, Becher MW, Wong PC, Zweier JL. Overexpression of human copper,zinc-superoxide dismutase (SOD1) prevents postischemic injury. Proc Natl Acad Sci U S A 95: 4556–4560, 1998.
3. Lei XG. In vivo antioxidant role of glutathione peroxidase: evidence from knockout mice. Methods Enzymol 347:213–225, 2002.
4. Fu Y, Cheng WH, Porres JM, Ross DA, Lei XG. Knockout of cellular glutathione peroxidase gene renders mice susceptible to diquat-induced oxidative stress. Free Radic Biol Med 27:605–611, 1999.
5. Ho YS, Magnenat JL, Bronson RT, Cao J, Gargano M, Sugawara M, Funk CD. Mice deficient in cellular glutathione peroxidase develop normally and show no increased sensitivity to hyperoxia. J Biol Chem 272:16644–16651, 1997.
6. Ho YS, Gargano M, Cao J, Bronson RJ, Heimler I, Hutz RJ. Reduced fertility in female mice lacking copper-zinc superoxide dismutase. J Biol Chem 273:7765–7769, 1998.
7. Kawase M, Murakami K, Fujimura M, Morita-Fujimura Y, Gasche Y, Kondo T, Scott RW, Chan PH, Wolin MS. Exacerbation of delayed cell injury after transient global ischemia in mutant mice with CuZn superoxide dismutase deficiency. Stroke 30:1962–1968, 1999.
8. Lee WM. Acetaminophen and the U.S. acute liver failure study group: lowering the risks of hepatic failure. Hepatology 40:6–9, 2004.
9. Gardner CR, Heck DE, Yang CS, Thomas PE, Zhang XJ, DeGeorge GL, Laskin JD, Laskin DL. Role of nitric oxide in acetaminophen-induced hepatotoxicity in the rat. Hepatology 27:748–754, 1998.
10. Hinson JA, Pike SL, Pumford NR, Mayeux PR. Nitrotyrosine-protein adducts in hepatic centrilobular areas following toxic doses of acetaminophen in mice. Chem Res Toxicol 11:604–607, 1998.
11. Knight TR, Ho YS, Farhood A, Jaeschke H. Peroxynitrite is a critical mediator of acetaminophen hepatotoxicity in murine livers: protection by glutathione. J Pharmacol Exp Ther 303:468–475, 2002.
12. Mirochnitchenko O, Weisbrot-Lefkowitz M, Reuhl K, Chen L, Yang C, Inouye M. Acetaminophen toxicity. Opposite effects of two forms of glutathione peroxidase. J Biol Chem 274:10349–10355, 1999.
13. Nakae D, Yamamoto K, Yoshiji H, Kinugasa T, Maruyama H, Farber JL, Konishi Y. Liposome-encapsulated superoxide dismutase prevents liver necrosis induced by acetaminophen. Am J Pathol 136:787–795, 1990.
14. Ferret PJ, Hammoud R, Tulliez M, Tran A, Trebeden H, Jaffray P, Malassagne B, Calmus Y, Weill B, Batteux F. Detoxification of reactive oxygen species by a nonpeptidyl mimic of superoxide dismutase cures acetaminophen-induced acute liver failure in the mouse. Hepatology 33:1173–1180, 2001.
15. Cheng W-H, Quimby FW, Lei XG. Impacts of glutathione peroxidase-1 knockout on the protection by injected selenium against the pro-oxidant-induced liver aponecrosis and signaling in selenium-deficient mice. Free Radic Biol Med 34:918–927, 2003.
16. Fang Y, Han SI, Mitchell C, Gupta S, Studer E, Grant S, Hylemon PB, Paul Dent. Bile acids induce mitochondrial ROS, which promote activation of receptor tyrosine kinases and signaling pathways in rat hepatocytes. Hepatology 40:961–971, 2004.
17. Kamata H, Honda S, Maeda S, Chang L, Hirata H, Karin M. Reactive oxygen species promote TNF[alpha]-induced death and sustained JNK activation by inhibiting MAP kinase phosphatases. Cell 120:649–661, 2005.
18. Gupta A, Rosenberger SF, Bowden GT. Increased ROS levels contribute to elevated transcription factor and MAP kinase activities in malignantly progressed mouse keratinocyte cell lines. Carcinogenesis 20:2063–2073, 1999.
19. Kaushal GP, Liu L, Kaushal V, Hong X, Melnyk O, Seth R, Safirstein R, Shah SV. Regulation of caspase-3 and -9 activation in oxidant stress to RTE by forkhead transcription factors, Bcl-2 proteins, and MAP kinases. Am J Physiol Renal Physiol 287:F1258–F1268, 2004.
20. Bae MA, Pie JE, Song BJ. Acetaminophen induces apoptosis of C6 Glioma cells by activating the c-jun NH2-terminal protein kinase-related cell death pathway. Mol Pharmacol 60:847–856, 2001.
21. Liu J, Li C, Waalkes MP, Clark J, Myers P, Saavedra JE, Keefer LK. The nitric oxide donor, V-PYRRO/NO, protects against acetaminophen-induced hepatotoxicity in mice. Hepatology 37:324–333, 2003.
22. Ray SD, Balasubramanian G, Bagchi D, Reddy CS. Ca2+-calmodulin antagonist chlorpromazine and poly(ADP-ribose) polymerase modulators 4-aminobenzamide and nicotinamide influence hepatic expression of BCL-XL and P53 and protect against acetaminophen-induced programmed and unprogrammed cell death in mice. Free Radic Biol Med 31:277–291, 2001.
23. Chiu H, Gardner CR, Dambach DM, Durham SK, Brittingham JA, Laskin JD, Laskin DL. Role of tumor necrosis factor receptor 1 (p55) in hepatocyte proliferation during acetaminophen-induced toxicity in mice. Toxicol Appl Pharmacol 193:218–227, 2003.
24. El-Hassan H, Anwar K, Macanas-Pirard P, Crabtree M, Chow SC, Johnson VL, Lee PC, Hinton RH, Price SC, Kass GEN. Involvement of mitochondria in acetaminophen-induced apoptosis and hepatic injury: Roles of cytochrome c, Bax, Bid, and caspases. Toxicol Appl Pharmacol 191:118–129, 2003.
25. Reid AB, Kurten RC, McCullough SS, Brock RW, Hinson JA. Mechanisms of acetaminophen-induced hepatotoxicity: role of oxidative stress and mitochondrial permeability transition in freshly isolated mouse hepatocytes. J Pharmacol Exp Ther 312:509–516, 2005.
26. Ray SD, Jena N. A hepatotoxic dose of acetaminophen modulates expression of BCL-2, BCL-X(L), and BCL-X(S) during apoptotic and necrotic death of mouse liver cells in vivo. Arch Toxicol 73:594–606, 2000.
27. Nicholson DW. Caspase structure, proteolytic substrates, and function during apoptotic cell death. Cell Death Differ 6:1028–1042, 1999.
28. Lawrence RA, Sunde RA, Schwartz GL, Hoekstra WG. Glutathione peroxidase activity in rat lens and other tissues in relation to dietary selenium intake. Exp Eye Res 18:563–569, 1974.
29. Lowry OH, Rosebrough NJ, Farr AL, Randall RJ. Protein measurement with the Folin phenol reagent. J Biol Chem 193:265–275, 1951.
30. Pierce RH, Franklin CC, Campbell JS, Tonge RP, Chen W, Fausto N, Nelson SD, Bruschi SA. Cell culture model for acetaminophen-induced hepatocyte death in vivo. Biochem Pharmacol 64:413–424, 2002.
31. Gujral JS, Knight TR, Farhood A, Bajt ML, Jaeschke H. Mode of cell death after acetaminophen overdose in mice: apoptosis or oncotic necrosis? Toxicol Sci 67:322–328, 2002.
32. Fu Y, Sies H, Lei XG. Opposite roles of selenium-dependent glutathione peroxidase-1 in superoxide generator diquat- and peroxynitrite-induced apoptosis and signaling. J Biol Chem 276:43004–43009, 2001.
33. Jiang D, Akopian G, Ho YS, Walsh JP, Andersen JK. Chronic brain

oxidation in a glutathione peroxidase knockout mouse model results in increased resistance to induced epileptic seizures. Exp Neurol 164:257–268, 2000.

34. Sies H, Sharov VS, Klotz LO, Briviba K. Glutathione peroxidase protects against peroxynitrite-mediated oxidations. A new function for selenoproteins as peroxynitrite reductase. J Biol Chem 272:27812–27817, 1997.
35. Beckman JS. Oxidative damage and tyrosine nitration from peroxynitrite. Chem Res Toxicol 9:836–844, 1996.
36. Bar-Peled O, Korkotian E, Segal M, Groner Y. Constitutive overexpression of Cu/Zn superoxide dismutase exacerbates kainic acid-induced apoptosis of transgenic Cu/Zn superoxide dismutase neurons. Proc Natl Acad Sci U S A 93:8530–8535, 1996.
37. Maundrell K, Antonsson B, Magnenat E, Camps M, Muda M, Chabert C, Gillieron C, Boschert U, Vial-Knecht E, Martinou JC, Arkinstall S. Bcl-2 undergoes phosphorylation by c-Jun N-terminal kinase/stress-activated protein kinases in the presence of the constitutively active GTP-binding protein Rac1. J Biol Chem 272:25238–25242, 1997.
38. Boulares AH, Zoltoski AJ, Stoica BA, Cuvillier O, Smulson ME. Acetaminophen induces a caspase-dependent and Bcl-XL sensitive apoptosis in human Hepatoma cells and lymphocytes. Pharmacol Toxicol 90:38–50, 2002.
39. Bajt ML, Knight TR, Farhood A, Jaeschke H. Scavenging peroxynitrite with glutathione promotes regeneration and enhances survival during acetaminophen-induced liver injury in mice. J Pharmacol Exp Ther 307:67–73, 2003.
40. Suzuki A, Tsutomi Y, Akahane K, Araki T, Miura M. Resistance to Fas-mediated apoptosis: activation of caspase 3 is regulated by cell cycle regulator p21WAF1 and IAP gene family ILP. Oncogene 17: 931–939, 1998.
41. Zandi E, Rothwarf DM, Delhase M, Hayakawa M, Karin M. The IkappaB kinase complex (IKK) contains two kinase subunits, IKKalpha and IKKbeta, necessary for IkappaB phosphorylation and NF-kappaB activation. Cell 91:243–252, 1997.